

# Synthesis and Characterization of a Novel Screen-Printed Modified Gold Electrode with Applications in Uranyl Ions Detection

LIANA ANICAI<sup>1</sup>, CRISTINA STOICA<sup>1</sup>, CRISTINA VLADUT<sup>1</sup>, ANDRADA NEGRU<sup>1,2</sup>, JEAN-MARIE TEULON<sup>3</sup>, MICHAEL ODORICO<sup>3</sup>, JEAN-LUC PELLEQUER<sup>3</sup>, PIERRE PAROT<sup>3</sup>, MARIUS ENACHESCU<sup>1\*</sup>

<sup>1</sup> Politehnica University of Bucharest, Center of Surface Science and Nanotechnology, 313 Splaiul Independentei, 060042, Bucharest, Romania

<sup>2</sup> University of Pitesti, 1 Târgul din Vale, 110040, Pitesti, Romania

<sup>3</sup> CEA, iBEB, Commissariat à l'énergie atomique et aux énergies alternatives, F-30207 Bagnols sur Céze, France

*The paper presents experimental results regarding the preparation and characterization of a novel screen-printed modified gold electrode through formation of a self-assembled monolayer involving mercapto-undecanoic acid (MUA), followed by the attachment of C-Reactive Protein (CRP), as a specific metal binding protein with a strong affinity to uranyl ions. The average grain size, roughness and profile height during the stepwise assembly of the layered functionalized electrode were determined by Atomic Force Microscopy. Raman spectroscopy has been also applied to get more evidence on the immobilization of uranyl ions onto the modified Au/MUA/CRP electrode. Comparative cyclic voltammograms of ferro/ferricyanide couple in buffer solution using bare Au, Au/MUA and Au/MUA/CRP electrodes showed the self-assembled monolayer formation and addition of stable thin protein layer. It was demonstrated that the Au/MUA/CRP electrode could be suitable for quantitative detection through EIS technique based on the proportional response of charge transfer resistance against uranyl ions concentration.*

*Keywords: modified gold electrode, self-assembled monolayer, uranyl ion, Raman spectroscopy, AFM, electrochemical response*

In the recent years, the development of monitoring capability of highly toxic components, including heavy metals ions became an important issue thanks to a greater awareness of their effects on the environmental components (water, air, soil) and on human health. Among them, a significant impact mainly on water and soil is related to uranium and its compounds, especially detected in industrial areas with nuclear activity (e.g., nuclear power plants), as well as in other fields currently using them during production processes or analysis, such as electron microscopy investigations of biological samples, materials for staining of ceramic products, geochemical exploration of uranium, etc. [1-3].

Uranium element presents various oxidation states (namely +2, +3, +4, +5 and +6), among them hexavalent form leading to the formation of uranyl ion,  $\text{UO}_2^{2+}$ , very stable and water soluble. This is why it has the highest probability to be transferred towards the environmental components, especially through wastewaters and consequently to significantly affect the human health. Uranyl ions may quickly pass through the gastrointestinal tract. Most uranyl is carried as soluble bicarbonate in the bloodstream while the remainder is bound to plasma proteins. Several investigations [4,5] reported that while about 60% of the uranyl amount is excreted within 24 h, approximately 25% was incorporated to bone. Currently, there are no validated methods able to allow the reducing of chronic effects of uranyl exposure, so that its early detection involving biosensing would be beneficial [5].

A variety of analytical methods to adequately detect the uranium species in water solutions have been reported, including: fluorimetry, ICP spectroscopy, XRF (X-ray Fluorescence Spectroscopy), optical methods, electrochemical methods such as: voltammetry, potentiometry,

differential pulse polarography, etc. [2,6,7 and included references]. Most of the analytical physical-chemical methods require complex and costly equipment and specific reagents. On the other hand, the electroanalytical techniques represent today very useful ones, due to their high sensitivity, selectivity and operation simplicity. In addition, they can be easily adapted to solve many analytical problems related to different compounds specificity, do not require expensive chemicals and allow the achievement of extremely low detection limits, of about  $10^{-8}$  –  $10^{-9}$  mol/L [1,3,8]. The most used electrochemical method to detect uranyl species is based on the stripping voltammetry, that allowed the obtaining of a detection limit of about  $2 \cdot 10^{-8}$  mol/L. To further improve the selectivity and detection limit, several agents have been introduced which facilitate a better adhesion of the complex to the electrode surface, such as: 2-thenoyltrifluoroacetone-tributylphosphine oxide, cupferron, 2,6-pyridinedicarboxylic acid, tiron or calixarens [1,8-10 and included references].

The electrochemical detection methods are usually based on the use of chemically modified electrodes that allow a high affinity to the uranyl ion while having a short time response and robustness. They also represent the main element during building of electrochemical sensors and biosensors.

The preparation of surface modified electrodes through self-assembled monolayers (SAMs) involving various thiol derivatives has attracted an increased interest in the past two decades, mainly for applications related to the electroanalytical detection [2,6,8,9,11-13]. The formed SAMs provide a convenient, flexible and easy system that allows the tailoring of the interfacial properties of metals, metal oxides and semiconductors. They are organic assemblies formed onto the surface of solids through

\* email: enachescu2007@gmail.com

adsorption of molecular constituents from liquid or gas phase. The adsorbate organizes spontaneously into the crystalline/semi-crystalline structure of the solid surface. The molecules or ligands that form SAMs have a chemical functionality, respectively they contain a "head-group" with a high affinity for a substrate. The most extensively investigated and used class of SAMs is derived from the adsorption of alkanethiols on Au, Ag, Pt, Cu and Hg electrodes. The high affinity of thiols for the surface of noble metals leads to the generation of well-defined organic surfaces with useful and highly alterable chemical functionalities located at the exposed interface [13 and included references]. Usually, the SAMs functionalized electrodes have been applied to electrochemically detect the alkaline and alkaline-earth metals cations, (e.g. Na<sup>+</sup>, K<sup>+</sup>, Li<sup>+</sup> and respectively, Ca<sup>2+</sup>, Ba<sup>2+</sup>) using electrochemical impedance spectroscopy and only few investigations discussed their involvement for heavy metals species detection, including uranyl ions [2,11 and included references].

The use of phosphate groups represents a promising route to build electrochemical sensors and biosensors for uranyl detection, due to their highly strong interaction with transition metal ions, especially UO<sub>2</sub><sup>2+</sup>. The SAMs may be functionalized either with phosphate/phosphine derivatives [2,9] or using DNA that further will interact with UO<sub>2</sub><sup>+</sup> through the existing phosphate skeleton [1,8].

In the last years several investigations used the metal-protein interaction in order to design electrodes for electrochemical detection of heavy metals. Generally, uranyl ions form coordination compounds with 5 or 6 acid donor ligands in horizontal plane. In the case of proteins, these ligands are provided by the oxygen atoms from carbonyl, carboxyl, phenolic or phosphoryl groups. It has been shown that the phenolic and phosphoryl groups in such organic complexes of uranyl ion present the shortest U-O distances, based on the analysis of the uranium-ligand bond length. Thus, these chemical groups are characterized by the strongest affinity towards uranyl. In addition, the affinity of uranyl ion against phosphate groups was also supported by the formation of several phosphate-uranyl minerals, as well as by the strong interaction between uranyl and phospholipids, phosphorylated proteins such as those present in the bacterial surface layer of *Bacillus sphaericus* JG-A12 [14-16]. Conroy *et al.* [5] reported the building of a biosensor based on UO<sub>2</sub><sup>2+</sup> binding protein using *Lysinibacillus sphaericus* JG-A12 S-layer protein tethered to gold electrodes.

The coordination properties of uranyl ion are relatively similar with those of calcium. Both metallic cations form preferentially electrostatic interactions with strong oxygen donor ligands and the preferred coordination geometry of Ca<sup>2+</sup>- seven ligands arranged in distorted octahedral or pentagonal bipyramidal structures – is similar to that found in the case of uranyl complexes. The reported results in [14,16,17] showed that uranyl ions can compete Ca<sup>2+</sup> ions in the formation of interactions with albumine or C reactive protein (CRP). Thus, Pible *et al.* [14] reported an apparent affinity of UO<sub>2</sub><sup>2+</sup> for native CRP of almost 100-fold higher than that of Ca<sup>2+</sup>, based on Surface Plasmon Resonance (SPR) investigations.

Preliminary investigations related to the fabrication and characterization of a novel uranyl binding protein based modified gold electrode suitable for electrochemical detection are presented in the present report, based on the use of a SAM-Protein (CRP)-Metal complex nanostructure.

## Experimental part

### Materials and reagents

Gold screen printed electrodes (Au-SPE) with Au working electrode (4 mm diameter), Au counter electrode and a silver pseudo-reference (220AT, from Dropsens-Spain) have been used. It is worth to mention that in the recent years, the chemical and electrochemical treatment of screen printed electrodes represent a novel promising route to develop (bio)chemical sensors for environmental, industrial and biomedical applications, due to their low cost and available large scale mass production [18].

All chemical reagents, respectively: mercapto-undecanoic acid (MUA), ethyl-N-[3-diethylaminopropyl] carbodiimide (EDC), *N*-hydroxysuccinimide (NHS); ethanolamine, Human C Reactive Protein (CRP), acetic acid, sodium acetate, phosphate-buffered saline (PBS), Tris-buffered saline, ethanol, uranyl acetate, potassium ferrocyanide and ferricyanide were of analytical grade and purchased from commercial providers (Sigma Aldrich, Pierce Biotechnology, R&D Systems Europe Lille France).

### Apparatus

The physico-chemical and morphological characterization of the SAM/CRP and UO<sub>2</sub><sup>2+</sup> modified Au electrode has been carried out using micro-Raman spectroscopy (Horiba LabRam HR 800 equipment, in which excitation was made by 633 nm wavelength laser light (He-Ne laser) and Atomic Force Microscopy (AFM) technique in tapping mode (home-built system controlled by commercial electronics (SPM1000 and PLLPro2 from RHK Technologies).

All electrochemical experiments have been performed in a 5 cm<sup>3</sup> cell, at room temperature (20±5°C), in stationary conditions, involving 10 mM [Fe(CN)<sub>6</sub>]<sup>3-/4-</sup> (1:1) solution prepared in acetate buffer of pH 6. The cyclic voltammetry (CV) and electrochemical impedance spectroscopy (EIS) measurements were made using a PARSTAT 4000 (Princeton Applied Research) electrochemical equipment. EIS spectra, recorded with 10 mV a.c. voltage within 10<sup>5</sup> Hz ÷ 10<sup>-1</sup> Hz frequency range, have been processed using ZView 2.9b software from Scribner Association Inc., Derek Johnson.

### Preparation of modified electrode

The gold electrodes have been initially subjected to a surface preparation step using an adapted procedure from Fischer *et al.* [19], as it follows:

- (i) sonication in ethanol for 5 min.;
- (ii) sonication in isopropilic alcohol for 5 min.;
- (iii) immersion in aqueous solution containing 50 mM KOH+25% H<sub>2</sub>O<sub>2</sub> for 10 min.;
- (iv) electrocycling in 50 mM KOH solution (50 mVs<sup>-1</sup>) from -0.2V to -1.2 V (Ag ref.).

The SAM has been prepared by dropping 20µL of 1mM MUA ethanolic solution on the gold electrode surface for 1h, followed by washing with ethanol and water. The surfaces have been incubated for 30 min. using 0.4 mg/mL EDC water solution and 0.6 mg/mL NHS solution, followed again by washing with 20 mM acetate buffer (pH 4.5). Then a drop of CRP solutions of 10 nM/100 nM/1 µM in 20 mM acetate buffer has been added on the SAM modified electrode surface and left overnight at 4°C. Another rinsing sequence has been applied using acetate buffer and 20 mM Tris buffer (pH 8). To block the unreacted carboxylic groups, a drop of 1M ethanolamine solution (pH 8.5) has been added for 10 min. A final rinsing with 20 mM PBS solution has been applied and stored at 4°C until use.

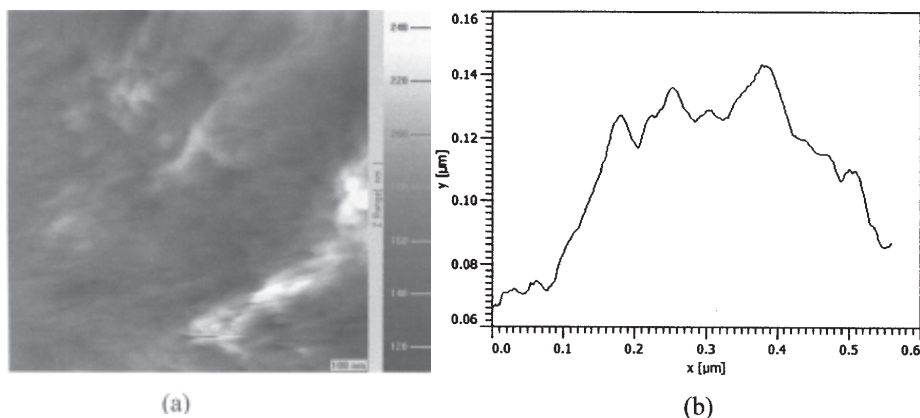


Fig.1. (a) AFM topography and (b) grain profile of the cleaned Au electrode (1  $\mu\text{m}$  x 1  $\mu\text{m}$ )

## Results and discussions

### AFM characterization

AFM microscopy has been involved to get more details regarding the surface structural characteristics of the chemically modified gold electrode at different stages of surface preparation: (i) SAM formation (Au/MUA), followed by (ii) CRP binding (Au/MUA/CRP) and finally (iii)  $\text{UO}_2^{2+}$  ions complexation (Au/MUA/CRP/ $\text{UO}_2^{2+}$ ).

Figure 1a illustrates the cleaned Au electrode surface, evidencing an uneven appearance at nanometric level, in agreement with the technical data provided by the manufacturer [20]. However, this roughness could contribute to a better adhesion of the further deposited layers, on one side, and these features could hinder an adequate inspection at nanometer level of the modified surfaces.

Considering the cross section shown in figure 1b, the average grain size was estimated to be around 60 nm, while the calculated RMS roughness (root mean squared roughness) was about 53.9 nm.

The SAM formation on the gold electrode involving MUA lead to a relatively homogenous surface, as shown in figure 2a, consisting of elongated and quite ordered structures, with an average grain size of around 40 nm (fig.2b). A RMS roughness of about 76.7 nm was estimated, with more than 20 nm higher than that of the cleaned electrode surface.

The AFM images captured after the immobilization of CRP involving 1mM solution onto the previously formed Au/MUA structure are presented in figure 3.

As a result of protein attachment, the previously evidenced SAM ordered structures were entirely covered.

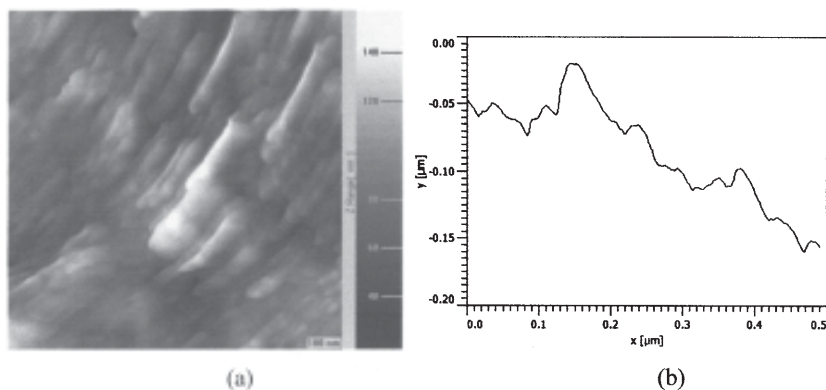


Fig.2. (a) AFM topography and (b) grain profile of the modified Au/MUA electrode (1  $\mu\text{m}$  x 1  $\mu\text{m}$ )

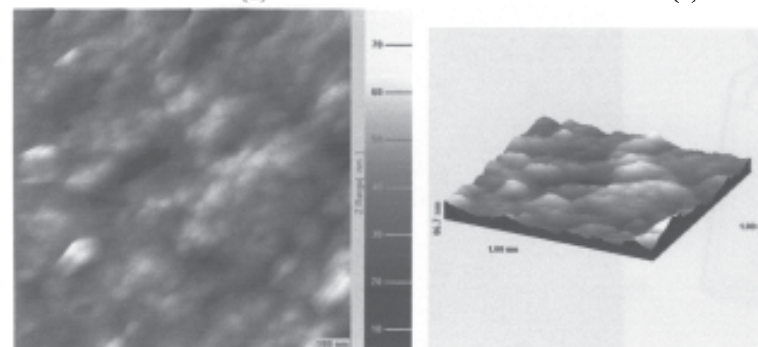


Fig.3. 2D (left) and 3D (right) AFM images for the modified Au/MUA/CRP electrode (1  $\mu\text{m}$  x 1  $\mu\text{m}$ )

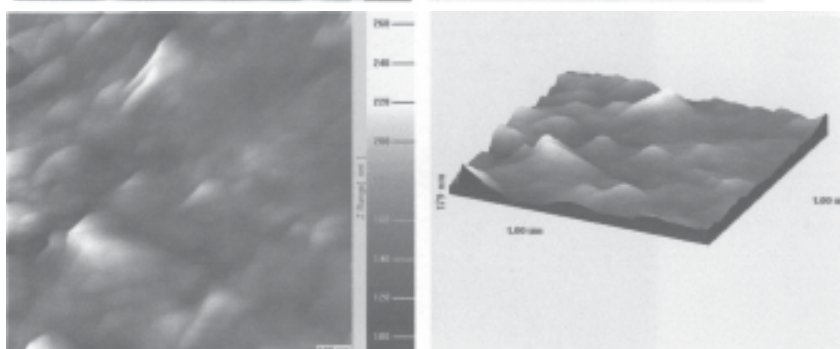


Fig.4. 2D (left) and 3D (right) AFM images for the modified Au/MUA/CRP/ $\text{UO}_2^{2+}$  electrode (1  $\mu\text{m}$  x 1  $\mu\text{m}$ )

Consequently, the addition of CRP on SAM surface determined a much smaller roughness (RMS 14.26 nm, maximum profile height 80-90 nm).

After the building of Au/MUA/CRP detection structure, the modified electrode has been subjected to chemical immersion in 0.01M uranyl acetate solution in acetate buffer pH 6, for 60 min. figure 4 shows the AFM images for the modified electrode surface after uranyl ion binding.

As shown in figure 4, the surface structure is quite similar to that evidenced after CRP immobilization. However, a slight increase of the RMS roughness up to about 56.2 nm and a maximum profile height of 180 nm were estimated, suggesting the uranyl ions coupling with coordination ligands of the protein. It should be mentioned that the roughness was determined not only by the size of the grains but by their surface structure, too.

### Raman spectroscopy

Micro-Raman spectroscopy has been also involved to get more evidence on the immobilization of uranyl ions onto the modified Au/MUA/CRP electrode. Therefore, Fig.5 presents an example of Raman spectrum recorded in the case of a modified Au/MUA/CRP electrode after chemical immersion for 20 min. in 10 mM uranyl acetate solution.

Usually, Raman peaks, located in the region from 785 to 910  $\text{cm}^{-1}$  are attributed to the  $\text{UO}_2^{2+}$  stretching vibrations. Bands at wavenumbers between 200-300  $\text{cm}^{-1}$  connected with the split doubly degenerate  $\nu_2(\delta)$  ( $\text{UO}_2$ ) bending vibrations and  $\delta$ ,  $\nu(\text{U-O}_{\text{ligand}})$  vibrations [21-23].

As can be seen in figure 5, the micro-Raman spectrum shows a distinct band at 834  $\text{cm}^{-1}$ , assigned to  $(\text{UO}_2)^{2+}(\nu_1)$  and a band at 267  $\text{cm}^{-1}$  assigned to the  $\nu_2(\delta)$  ( $\text{UO}_2$ )<sup>2+</sup> [21,22]. The shoulder at 1058  $\text{cm}^{-1}$  may be attributed to the CH groups from organic structure while the band at 2151  $\text{cm}^{-1}$  to C=N, C=C bonds from the protein composition. The bands in the region of 400-600  $\text{cm}^{-1}$  might be assigned to C-S and S-S bonds from MUA and/or CRP composition [24].

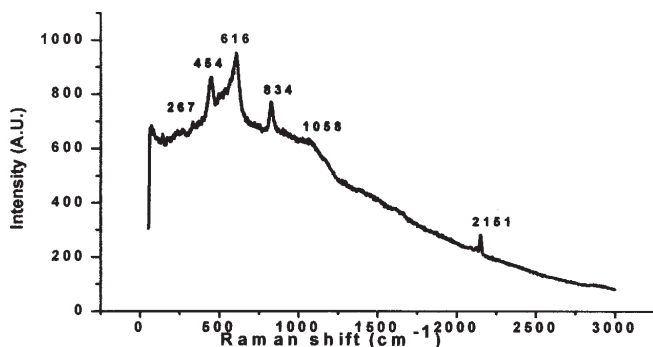


Fig.5. Micro-Raman spectrum of the Au/MUA/CRP electrode after chemical immersion for 20 min. in 10 mM uranyl acetate solution

### Cyclic voltammetry

The stepwise assembly of the layered functionalized electrode was traced by cyclic voltammetry and electrochemical impedance spectroscopy in the presence of 10 mM  $[\text{Fe}(\text{CN})_6]^{3-/4}$  couple (1:1) in buffer solution as redox probe. The electrochemical response has been investigated after each applied layer to confirm the assembly process.

Figure 6 shows the recorded cyclic voltammograms of the bare cleaned Au electrode (curve a) and of modified electrode with MUA based SAM (Au/MUA).

It should be mentioned that an uncontaminated Au surface is very important for the adequate chemisorption of thiol derivatives and self-assembled monolayer formation. The cyclic voltammogram of Au electrode (curve

a) evidences a potential difference between redox peaks of about 80 mV, with a relatively equal amplitude of the current, suggesting a satisfactory cleaning process.

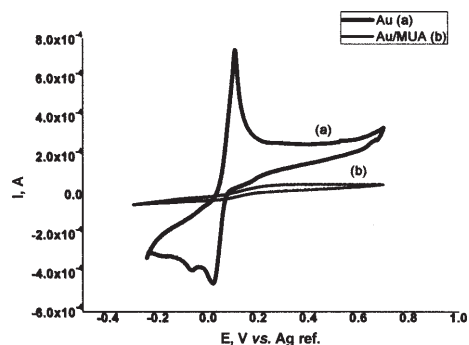


Fig.6. Cyclic voltammograms recorded in 10 mM  $[\text{Fe}(\text{CN})_6]^{3-/4}$  (1:1) solution for: (a) Au and (b) Au/MUA electrodes (scan rate: 50  $\text{mVs}^{-1}$ ;  $S_{\text{WE}} = 0.125 \text{ cm}^2$ )

When 1mM MUA solution has been applied onto Au electrode surface, stable and strong S-Au bonds were formed. This process has been confirmed by a significant decrease of peak currents (curve b), determined by the inhibition of the electronic transfer between the electroactive species and electrode, due to the presence of the MUA based monolayer.

After that, the modified Au/MUA electrode was subjected to CRP attachment, involving solutions with various protein concentrations in the range of 10 nM ÷ 1  $\mu\text{M}$ . Changes in interfacial properties by adding a new thin protein layer are evidenced in the recorded voltammograms from figure 7 by a slight decrease of electrochemical area and shift of anodic and cathodic potential (curve b).

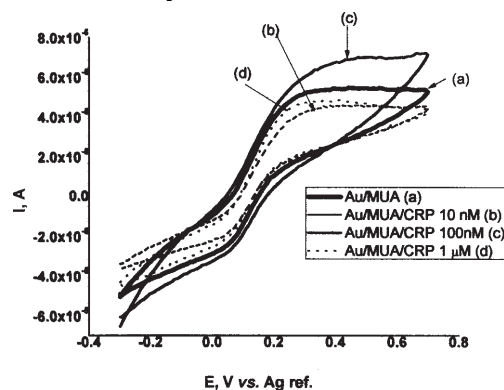


Fig.7. Cyclic voltammograms recorded in 10 mM  $[\text{Fe}(\text{CN})_6]^{3-/4}$  (1:1) solution for (a) Au/MUA and (b-d) Au/MUA/CRP modified electrodes involving different CRP concentrations: (b) 10 nM; (c) 100 nM and (d) 1  $\mu\text{M}$  (scan rate: 50  $\text{mVs}^{-1}$ ;  $S_{\text{WE}} = 0.125 \text{ cm}^2$ )

The use of more concentrated CRP solutions not necessarily facilitates formation of more compact films, as illustrated in curves (c) and (d) from figure 7. This behaviour should be related to the possible occurrence of some secondary reactions between protein groups with no SAM attachment, thus leading to incomplete surface covering which further may allow the electronic transfer of ferri/ferrocyanide redox couple [25]. One may thus assume that in order to obtain a coherent protein structure able to entirely cover the electrode surface, less concentrated CRP solutions, of 10 nM may be applied.

Then the modified Au/MUA/CRP electrodes have been immersed in 10 mM  $\text{UO}_2^{2+}$  solution for different accumulation periods followed by the analysis of electrochemical response in the presence of ferri/ferrocyanide redox couple.

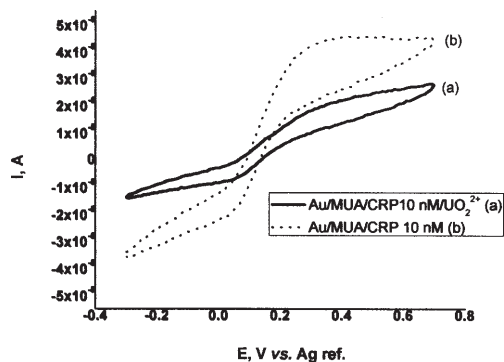


Fig.8. Comparative cyclic voltammograms recorded in 10 mM  $[\text{Fe}(\text{CN})_6]^{3-/4-}$  (1:1) solution for Au/MUA/CRP modified electrode after immersion in: (a) 10 mM  $\text{UO}_2^{2+}$  solution and (b) pure acetate buffer solution pH 6, for 22 min. (scan rate: 50 mVs<sup>-1</sup>;  $S_{\text{WE}} = 0.125 \text{ cm}^2$ )

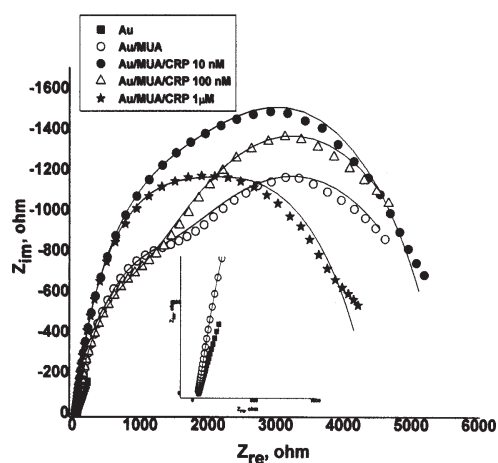


Fig.9. Nyquist plots of EIS spectra recorded on bare Au, Au/MUA and Au/MUA/CRP modified electrodes in 10 mM  $[\text{Fe}(\text{CN})_6]^{3-/4-}$  (1:1) solution at  $E = +0.13\text{V}/\text{Ag ref.}$  (solid lines are the fit to the measured points using the inserted equivalent circuit)

Figure 8 presents an example of the recorded voltammograms for the modified Au/MUA/CRP electrode after immersion in 10 mM  $\text{UO}_2^{2+}$  solution for 22 min.

As figure 8 shows, the current maxima of ferri/ferrocyanide redox couple after electrode incubation in  $\text{UO}_2^{2+}$  based solution have significantly smaller values. This result suggests that conditioning of the Au/MUA/CRP modified electrode in 10 mM  $\text{UO}_2^{2+}$  (curve a) blocked the electron transfer between the redox couple and the electrode. Uranyl ions have been adsorbed onto CRP surface forming strong interactions, in agreement with literature data which demonstrated a strong affinity of CRP protein for uranyl ions [14,16,17].

#### Electrochemical impedance spectroscopy

The EIS represents a powerful, non-destructive technique to get information on the processes occurring at the electrode/film interface taking into consideration the produced modifications through adsorption of various investigated species onto electrode.

Therefore, EIS measurements were performed to trace the events during formation of the different layers onto the gold electrode.

Figure 9 shows the recorded EIS spectra as Nyquist plots for bare Au electrode and upon the assembly of the different layers on the electrode.

The bare Au electrode exhibits an almost straight line that is characteristic to a diffusion limiting electron transfer process. Assembly of the mercapto-undecanoic acid (MUA) monolayer on the electrode surface generates a layer on

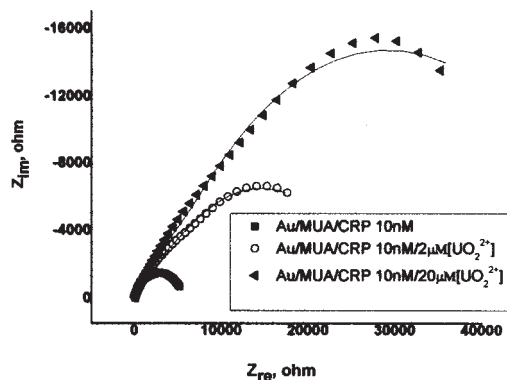


Fig.10. Nyquist plots of the recorded EIS spectra on Au/SAM/CRP electrode after 20 min. immersion in solutions having various  $\text{UO}_2^{2+}$  concentrations (measurements recorded in the presence of 10 mM  $[\text{Fe}(\text{CN})_6]^{3/4-}$  (1:1) solution)

the electrode that introduces a barrier to the interfacial electron-transfer, evidenced by the presence of a semicircle. In addition, the presence of two time constants is noticed, suggesting formation of a more complex structure consisting of a relatively porous region and a more compact one, which may be assigned to a different ordering of the monolayer on the electrode surface. The attachment of the CRP layer adds a supplementary barrier that influences the interfacial electronic transfer at the interface, materialized by an increase of the semicircle diameter related to the charge transfer resistance. Again, the Au/MUA/CRP modified electrode involving 10 nM CRP solutions showed the highest charge transfer resistance, in agreement with the obtained results from cyclic voltammetry investigations.

The affinity of the Au/MUA/CRP modified electrode towards uranyl ion allows its impedimetric detection. Figure 10 presents an example of the recorded EIS spectra for the Au/MUA/CRP 10 nM modified electrode after immersion for 20 min. in  $\text{UO}_2^{2+}$  solutions having concentrations in the range of 2  $\mu\text{M}$  – 10mM.

The increase in the uranyl ion concentration results in larger semicircle diameters in the Nyquist plots, implying higher values of charge transfer resistance ( $R_{ct}$ ). By changing uranyl ion concentration from 2  $\mu\text{M}$  to 20  $\mu\text{M}$ , the  $R_{ct}$  value increased from 23125  $\Omega$  to 50113  $\Omega$ , respectively, suggesting an enhancement of the electrical insulation of the electrode. This behavior evidenced a dependence of  $R_{ct}$  against uranyl content in the solution. This phenomenon is closely related to the strong affinity of CRP protein for uranyl ions.

The obtained preliminary results provide promising premises in order to build a novel sensor for electrochemical detection of uranyl ions, with a better stability and robustness.

#### Conclusions

A novel screen-printed modified gold electrode has been proposed through formation of a self-assembled monolayer involving mercapto-undecanoic acid, followed by the attachment of C Reactive Protein, as a specific metal binding protein with a strong affinity to uranyl ions.

The stepwise assembly of the layered functionalized electrode has been traced involving AFM microscopy. It was shown that self-assembled monolayer formation on the electrode surface determined a relatively homogenous surface, consisting in elongated structures with an average grain width of approx. 40 nm and RMS roughness of about 76 nm. The addition of the specific metal binding protein on SAM surface determined a much smaller roughness

(RMS roughness of 14.26 nm and maximum profile height of 80-90 nm).

The electrochemical investigations evidenced the formation of physically and chemically stable modified surfaces. The modified gold electrode involving C Reactive Protein showed a good affinity towards uranyl ions. Thus it could be suitable for quantitative detection through EIS technique based on the proportional response of charge transfer resistance against uranyl ions concentration.

Additional experiments to optimize the electrochemical response and selectivity of the proposed modified electrode are planned for future investigations.

*Acknowledgements: The funding from IFA-CEA Scientific Cooperation Program, ACHEME project, Research Contract C2-08/01.03.2012 is gratefully acknowledged.*

## References

1. ZIOLKOWSKI, R., GORSKI, L., OSZWALDOWSKI, S., MALINOWSKA, E., *Anal.Bioanal.Chem.*, 402, no.7, 2012, p. 2259
2. SHERVEDANI, R.K., MOZAFFARI, S.A., *Anal.Chim.Acta*, 562, no.2, 2006, p. 223
3. SHRIVASTAVA, A., SHARMA, J., SONI, V., *Bull.Fac.Pharm. Cairo Univ.*, 51, no.1, 2013, p. 113
4. KLAASSEN, C.D., *Casarett and Doull's Toxicology*, 7-th Ed., McGraw-Hill, New York, NY USA, 2008, p.971
5. CONROY, D.J.R., MILLNER, P.A., STEWART, D.I., POLLMANN, K., *Sensors*, 10, no.5, 2010, p. 4739
6. BANERJEE, R., KATSENOVICH, Y., LAGOS, L., SENN, M., NAJA, M., BALSAMO, V., PANNELL, K.H., LI, C.-Z., *Electrochim.Acta*, 55, no.27, 2010, p. 7897
7. DIMOVASILIS, P.A., PRODROMIDIS, M.I., *Sens.Actuators B.*, 156, no.2, 2011, p. 689
8. POURBEYRAM, S., SHERVEDANI, R.K., *Bioelectrochem.*, 92, 2013, p. 27
9. BECKER, A., TOBIAS, H., MANDLER, D., *Anal.Chem.*, 81, no.20, 2009, p. 8627
10. ANSOBORLO, E., PRAT, O., MOISY, P., DEN AUWER, C., GUILBAUD, P., CARRIERE, M., GOUGET, B., DUFFIELD, J., DOIZI, D., VERCOUTER, T., MOULIN, C., MOULIN, V., *Biochimie*, 88, no.11, 2006, p. 1605
11. SHERVEDANI, R.K., MOZAFFARI, S.A., *Surf.Coat.Technol.*, 198, no.1-3, 2005, p. 123
12. CHEN, Y., YANG, C., WANG, F.B., *Electrochim.Acta*, 55, no.12, 2010, p. 3951
13. LOVE, J. C., ESTROFF, L. A., KRIEBEL, J.K., NUZZO, R.G., WHITESIDES, G. M., *Chem. Rev.*, 105, no.4, 2005, p. 1103
14. PIBLE, O., VIDAUD, C., PLANTEVIN, S., PELLEQUER, J.-L., QUEMENEUR, E., *Prot. Sci.*, 19, no.11, 2010, p. 2219
15. MERROUN, M.L., RAFF, J., ROSSBERG, A., HENNIG, C., REICH, T., SELENSKA-POBELL, S., *Appl. Environ. Microbiol.*, 71, no.9, 2005, p. 5532-5543.
16. PARDOUX, R., SAUGE-MERLE, S., LEMAIRE, D., DELANGLE, P., GUILLOREAU, L., ADRIANO, J.-M., BERTHOMIEU, C., *Modulating Uranium Binding Affinity in Engineered Calmodulin EF-Hand Peptides: Effect of Phosphorylation*, *PLoS ONE*, 7(8), 2012, e41922, doi:10.1371/journal.pone.0041922
17. MONTAVON, G., APOSTOLIDIS, C., BRUCHERTSEIFER, F., REPINC, U., MORGENSTERN, A., *J. Inorg. Biochem.*, 103, no.12, 2009, p. 1609
18. DUTU, G., TERTIS, M., SANDULESCU, R., CRISTEA, C., *Rev. Chim.(Bucharest)*, 65, no.2, 2014, p. 142
19. FISCHER, L. M., TENJE, M., HEISKANEN, A.R., MASUDA, N., CASTILLO, J., BENTEN, A., ÉMNEUS, J., JAKOBSEN, M.H., BOISEN, A., *Microelectron. Eng.*, 86, no.4-6, 2009, p. 1282
- 20.\*\*\* [http://www.dropsens.com/en/pdfs\\_productos/new\\_brochures/gold\\_electrodes.pdf](http://www.dropsens.com/en/pdfs_productos/new_brochures/gold_electrodes.pdf)
21. FROST, R., CEJKA, J., WEIER, M., AYOKO, G., *J. Raman Spectrosc.*, 37, no.12, 2006, p. 1362
22. FROST, R.L., ČEJKA, J., WEIER, M.L., MARTENS, W., KLOPPROGGE, J.T., *Spectrochim. Acta Part A*, 64, no.2, 2006, p. 308
23. STEFANIAK, E.A., ALSECZ, A., FROST, R., SAJÓ, I.E., MÁTHÉ, Z., TÖRÖK, S., WOROBIEC, A., VAN GRIEKEN, R., *J. Hazard. Mater.*, 168, no.1, 2009, p. 416
24. SCHWARTZ, D.T., *Raman Spectroscopy: Introductory Tutorial*, available at <https://depts.washington.edu/ntuf/facility/docs/NTUF-Raman-Tutorial.pdf>
25. SILVA, M.M.S., CAVALCANTI, I.T., BARROSO, M.F., SALES, M.G., DUTRA, R.F., *J.Chem.Sci.* 122, no.6, 2010, p. 911

Manuscript received: 5.02.2015